crystals

MDPI

Article

General Properties of Conventional and High-Temperature Superconductors

Vasily R. Shaginyan [1,2,*], Alfred Z. Msezane [2] and Stanislav A. Artamonov [1]

[1] Petersburg Nuclear Physics Institute Named by B.P. Konstantinov of National Research Centre "Kurchatov Institute", Gatchina 188300, Russia; artamonov_sa@pnpi.nrcki.ru
[2] Department of Physics, Clark Atlanta University, Atlanta, GA 30314, USA; amsezane@cau.edu
* Correspondence: vrshag@thd.pnpi.spb.ru

Abstract: In our review, we analyze the scaling of the condensation energy E_Δ divided by γ, $E_\Delta/\gamma \simeq N(0)\Delta_1^2/\gamma$, and quasiparticles of both conventional and unconventional superconductors, where $N(0)$ is the density of states at zero temperature $T = 0$, Δ_1 is the maximum value of the superconducting gap, and γ is the Sommerfeld coefficient. It is shown that Bogoliubov quasiparticles act in superconducting states of unconventional and conventional superconductors. At the same time, quasiparticles are also present in the normal state of unconventional superconductors. We briefly describe the difference between unconventional superconductors and conventional ones, such as the resistivity in normal states and the difference in superfluid density in superconducting states. For the first time, we theoretically show that the universal scaling of $E_\Delta/\gamma \propto T_c^2$ applies equally to both conventional and unconventional superconductors. Our consideration is based on two experimental facts: Bogoliubov quasiparticles act in conventional and non-conventional superconductors and the corresponding flat band is deformed by the non-conventional superconducting state. As a result, our theoretical observations based on the theory of fermion condensation agree well with the experimental facts.

Keywords: quantum phase transition; flat bands; high-Tc superconductivity

PACS: 74.25.Bt; 74.72.-h; 64.70.Tg

Citation: Shaginyan, V.R.; Msezane, A.Z.; Artamonov, S.A. General Properties of Conventional and High-Temperature Superconductors. *Crystals* **2024**, *14*, 826. https://doi.org/10.3390/cryst14090826

Academic Editor: Omar Chmaissem

Received: 9 August 2024
Revised: 11 September 2024
Accepted: 19 September 2024
Published: 21 September 2024

1. Introduction

It is generally accepted that conventional superconductors have nothing in common with unconventional superconductors, since unconventional superconductors are metals with flat bands [1] in the absence of quasiparticles; see, e.g., [2,3]. On the other hand, experimental facts show that both types of superconductors have common properties: they have quasiparticles and exhibit the common scaling behavior of the scaled condensation energy E_Δ/γ; see, for example, [4–7]; while the corresponding flat bands of unconventional superconductors are deformed by the superconducting state, which makes unconventional superconductors similar to ordinary superconductors [8,9]. A universal scaling law has been discovered for the scaled condensation energy E_Δ/γ across a wide range of classes of superconductors [5], and this universal scaling law has not yet been explained. Thus, these facts pose a challenging puzzle for condensed matter researchers. As a result, the problem of identifying a theoretically justified, experimentally observed scaled condensation energy E_Δ/γ, applicable to conventional and non-traditional superconductors, becomes acute [5]. Our theoretical consideration is based on the experimental paper that examines a representative subset of cuprates under optimal doping without any pseudogap [5]. We assume that our consideration is also applicable to graphene, since it has flat bands that form its typical behavior observed in other unconventional superconductors; see [1,9–14] and Figures 5 and 6 of Ref. [5].

The flat band problem could have been solved many years ago when the Landau Fermi liquid (LFL) theory was developed [15]. As known, it deals with energy functionals $E_0[n(\mathbf{p})]$ in the functional space $[n]$ of quasiparticle distributions $n(\mathbf{p})$ located in $[n]$ between 0 and 1. This theory is based on assumption that the single particle spectrum of a normal Fermi liquid is similar to that of an ideal Fermi gas, differing from the latter in the value of the effective mass M^*. At temperature $T = 0$, in homogeneous isotropic matter, the LFL ground state quasiparticle distribution is the Fermi step function $n_F(p) = \theta(p - p_F)$. Quasiparticles fill the Fermi sphere up to the same radius $p_F = (3\pi^2\rho)^{1/3}$ (ρ is the number density and p_F is the Fermi momentum) as noninteracting particles (the Landau–Luttinger theorem [15]). From the mathematical point of view, in the LFL theory, the minimum of $E_0[n]$ is supposed to always lie at a boundary point n_F of the space $[n]$. This assumption remains valid as long as the necessary stability condition

$$\delta E_0 = \int (\varepsilon[\mathbf{p}, n(\mathbf{p}, T = 0)] - \mu)\delta n(\mathbf{p}, T = 0)\frac{d^3p}{(2\pi)^3} > 0, \tag{1}$$

is fulfilled. Here, $\varepsilon[\mathbf{p}, n(\mathbf{p})] = \delta E_0[n]/\delta n(\mathbf{p})$ is the quasiparticle energy, $n(\mathbf{p})$ is the quasiparticle distribution function, and μ is the chemical potential. The stability condition requires that the change in $E_0[n]$ for any admissible variation in n_F holds. Thus, it is the violation of the condition given by Equation (1) that results in the rearrangement of the distribution $n_F(\mathbf{p})$. The quasiparticle distribution function $n(\mathbf{p})$ is constrained by the Pauli principle $1 \geq n(\mathbf{p}) \geq 0$. As a result, there are two classes of solutions of Equation (1). One class forming flat bands is

$$\varepsilon(p) = \mu; \text{ if } 1 > n_0(\mathbf{p}) > 0 \text{ in } p_i < p < p_f, \tag{2}$$

which is valid if the special solution $n_0(\mathbf{p})$ becomes $1 > n_0(\mathbf{p}) > 0$ in some region $p_i < p_F < p_f$ [16–19]. The other conventional class is defined by $\delta n(\mathbf{p}) = 0$, with $n(\mathbf{p}) = 0$ or $n(\mathbf{p}) = 1$, that is, $n(\mathbf{p}) = n_F(\mathbf{p})$ [15].

Flat bands, now observed in many strongly correlated Fermi systems [1,13], first emerged as a mathematical curiosity [16], and now, represent a rapidly expanding and dynamic field with countless applications; see, e.g., [1,12,13,18–22]. High-T_c superconductors represent a wide class of strongly correlated Fermi systems, exhibiting the non-Fermi liquid (NFL) behavior defined by flat bands; see, e.g., [13,18–22]. As a result, one can expect that unconventional superconductors have nothing in common with conventional superconductors. For example, in the case of unconventional superconductors, the critical temperature is [13,16,19–22]

$$T_c \propto \Delta_1 \propto \lambda_0, \tag{3}$$

rather than being $T_c \propto \exp(-1/\lambda_0 N(0))$, where λ_0 is the superconducting coupling constant, Δ_1 is the maximum value of the superconducting gap, and $N(0)$ is the density of states at the Fermi surface at $T = 0$ [23,24]. However, in both conventional and unconventional superconductors, the condensation energy exhibits universal scaling behavior, $E_\Delta/\gamma \simeq N(0)\Delta_1^2/\gamma \propto T_c^2$, as follows from experimental facts [5].

In our review, we analyze both unconventional superconductors and conventional ones, and demonstrate that both of them exhibit the common universal scaling of the condensation energy E_Δ/γ, $E_\Delta/\gamma \simeq N(0)\Delta_1^2/\gamma$.

In Section 2, we consider the superconducting state with a flat band generated by fermion condensation (FC) at $T = 0$.

Section 3 is devoted to quasiparticles in systems with FC. We show that quasiparticles of unconventional superconductors become heavy but do not die.

Section 4 concentrates on superconducting with FC at finite temperatures.

In Section 5, for the first time, we explain that the universal scaling of $E_\Delta/\gamma \propto T_c^2$ applies equally to conventional and unconventional superconductors. Our results are in good agreement with experimental facts [5]. This observation suggests that the FC superconducting state is Bardeen–Cooper–Schrieffer (BCS)-like and suggests the fundamental

applicability of the BCS formalism [23] to describe some properties of the superconducting state, as predicted in [18,25]. Our analysis is made within the framework of the fermion condensation (FC) theory based on the topological fermion condensation quantum phase transition (FCQPT) that forms flat bands and leads to the universal scaling behavior of the thermodynamic and transport properties of HF metals [12,16,18].

Section 6 is devoted to the summary of the main results of our review.

2. Superconducting Systems with the FC State at $T = 0$

We suggest that efficient particle–particle interactions in superconducting systems with FC are attractive. We note that a strong repulsion in the particle–hole channel, inherent in the systems with FC, coexists with the attraction in the particle–particle channel. For example, the electron–electron attractive interaction arises in solids due to the phonon exchange. In a superconducting electron (hole) liquid, E_0 is the functional of two order parameters $n(\mathbf{p}) =< a^+_{\mathbf{p},\beta} a_{\mathbf{p},\beta} >$ and $\kappa(\mathbf{p}) =< a^+_{\mathbf{p},\beta} a^+_{-\mathbf{p},-\beta} >= \sqrt{n(\mathbf{p})(1-n(\mathbf{p}))}$. At $T = 0$, the variational derivative $\delta E_0[n(p), \kappa(p)]/\delta n(p) = 0$ reads

$$\xi(p) - \frac{\Delta(p)(1-2n(p))}{\sqrt{n(p)(1-n(p))}} = 0. \tag{4}$$

Here, E_0 is the ground state energy of the electron liquid, being the exact functional of the order parameter of the superconducting state $\kappa(\mathbf{p})$ and quasiparticle occupation numbers $n(\mathbf{p})$ [18,26]. The single-particle energy $\xi(p) = \varepsilon(p) - \mu$, with $\varepsilon(p) = \delta E_0/\delta n(p)$, while $\Delta(p) = -\delta E_0/\delta\kappa(p)$, and $\kappa(p) = \sqrt{n(p)(1-n(p))}$ is the superconducting order parameter at $T = 0$. The BCS equations read [23,24]

$$n(p) = \frac{1}{2}\left[1 - \frac{\xi(p)}{E(p)}\right], \quad E(p) = \sqrt{\xi(p)^2 + \Delta^2(p)}, \quad \kappa(p) = \frac{\Delta(p)}{2E(p)}. \tag{5}$$

In the BCS theory, $\kappa(p) \to 0$ while $\Delta \to 0$. However, there exist entirely different solutions with $\kappa \neq 0$ even if $\Delta \to 0$. Indeed, for $\Delta \to 0$, while $\kappa \neq 0$, the second term in Equation (4) vanishes, and again we arrive at Equation (2). Thus, such solutions describe superconducting states of the system with FC since the order parameter $\kappa \neq 0$ at the finite region $p_i < p < p_f$ [18,27,28]. Since $\Delta/\varepsilon^0_F << 1$, one can write $E_0[n(p), \kappa(p)] = E_0[n(p)] - \mu N + \delta E_s[\kappa(p)]$, where

$$\delta E_s = \frac{1}{2}\int\int \lambda_0(\mathbf{p}, \mathbf{p}_1)\kappa(\mathbf{p})\kappa(\mathbf{p}_1)\frac{d^3p d^3p_1}{(2\pi)^6}. \tag{6}$$

Here, ε^0_F is the Fermi energy. Then, in the case of s-pairing, the gap $\Delta(p)$ is given by

$$\Delta(p) = -\int \lambda_0(p, p_1)\sqrt{n(p_1)(1-n(p_1))}\frac{p_1^2 dp_1}{4\pi^2}, \tag{7}$$

where λ_0 is the zero harmonics of $\lambda_0(\mathbf{p}, \mathbf{p}')$ over the angle between $\mathbf{p}$ and $\mathbf{p}'$. Then, pairing forces influence FC little and replacing $n(p, T)$ in Equation (7) by $n_0(p)$ we obtain

$$\Delta_0(p) = -\int \lambda_0(p, p_1)\sqrt{n_0(p_1)(1-n_0(p_1))}\frac{p_1^2 dp_1}{4\pi^2}. \tag{8}$$

Here, $\kappa_0(p)$ reads

$$\kappa_0(p) = \sqrt{n_0(p)(1-n_0(p))} \tag{9}$$

As a result, we can define the density of the superconducting electrons n_{FC}:

$$n_{FC} \simeq \int \kappa_0(\mathbf{p})\frac{d\mathbf{p}}{(2\pi)^3}. \tag{10}$$

Substituting Equation (8) into Equations (4) and (5), one finds that in the FC region

$$\xi_0(p) = \frac{\Delta_0(p)(1-2n_0(p))}{\sqrt{n_0(p)(1-n_0(p))}}; \quad E_0(p) = \frac{|\Delta_0(p)|}{2\kappa_0(p)}. \tag{11}$$

The next step is adding integration outside of the FC region, e.g.,

$$\Delta_1(p) = \Delta_0(p) - \int \lambda_0(p,p_1)\theta(p_1)\frac{\Delta_0(p_1)}{E_0(p_1)}\frac{p_1^2 dp_1}{4\pi^2}, \tag{12}$$

where $\theta(p) = 0$ within the region of FC. The integral term, which diverges logarithmically in BCS theory, now represents a correction of the order of $\lambda_0^2 \ln\lambda_0$ to $\Delta \sim \lambda_0$, which leads to the suppression of the isotope effect in T_c. We see that the order parameter $\kappa_0(p)$ is non-zero even if $\Delta_1 = 0$. In other words, even in the absence of pairing interaction, if the FC situation prevails, the system goes into a state with spontaneous gauge breaking [18,28], which is traditionally associated with superconductivity. We also see that the gap Δ is linear in the coupling constant λ_0. This is in contrast to the normal BCS case, where the superconducting gap is exponentially small. Since $T_c \sim \lambda_0$, even the weak coupling limit, e.g., the attraction of phonons in the particle–particle channel with $L = 0$, is sufficient to provide a fairly high T_c [13,16,18,22,27,28]. On the other hand, when λ_0 becomes repulsive, the components of λ_L with $L = 1$ or $L = 2$ can be attractive, giving rise to pairing with non-zero L. Neutron stars are an example of such attraction: in them, s-pairing dies at $p_F \simeq 1.7\ fm^{-1}$, while p-pairing persists up to $p_F \simeq 4\ fm^{-1}$ [29]. Typically, the gap at $L \neq 0$ is suppressed compared to the s case. In systems with FC, there is no such suppression. The entropy S of a superconducting fluid with FC, S, vanishes at $T \to 0$, since $\Delta_1 \propto \lambda_0$, and if λ_1 is assumed to be infinitely small, then the entropy $S \to 0$ corresponds to the BCS theory.

3. Validity of the Quasiparticle Pattern

3.1. Finite Systems

The quasiparticle pattern [15] we proceeded from is applicable provided the width of $\gamma_{FC}(T)$ of the relevant single-particle states (in our case, the FC) does not exceed the energy $\varepsilon(p)$. First, we show that it is the inter-particle interaction that gives rise to the FC state. In this case, the resulting flat bands become susceptible to external influences generated by magnetic fields, pressure, temperature, etc., as well as to phase transitions occurring in the system under consideration. This observation is in good agreement with experimental facts [18]. Flat bands can emerge due to geometrical reasons and their properties would be different from those driven by interaction; see, e.g., [30,31]. To consider the flat bands caused by interactions, it is useful to start with a finite system that has non-degenerate single-particle states; that is, the low-lying states are separated from each other and do not decay at all. However, the interaction causes the single-particle states to collapse into the FC state. To give an example of FC in finite systems, consider a spherical atomic nucleus with closed shells and add $K >> 1$ particles to it; then, the energy E_0 change in the system is given by Equation [28]:

$$\delta E_0 = \Sigma_{\lambda,\lambda_1}\left(\varepsilon^o_\lambda \delta n_\lambda \delta_{\lambda,\lambda_1} + \frac{1}{2}\Gamma^{\lambda_1,\lambda_1}_{\lambda,\lambda}\delta n_\lambda \delta n_{\lambda_1}\right). \tag{13}$$

The levels are degenerate with respect to the magnetic quantum number m. The energies ε^o_λ (where $\lambda = n, l, j, m$) are calculated in a closed-shell nucleus. The interaction amplitude Γ contains all re-scattering processes, taking place in a finite nucleus. It is not much different from the static scattering amplitude calculated in infinite nuclear matter. The case with only two terms with $j_i >> 1$ in the sum (13), for which $n_1 + n_2 = K < (2j_{min} + 1)$, is especially clear. Then, Equation (13) takes the form

$$\delta E_0 = \varepsilon^o_1 n_1 + \varepsilon^o_2 n_2 + \frac{1}{2}D_1 n_1^2 + U n_1 n_2 + \frac{1}{2}D_2 n_2^2, \tag{14}$$

and the single-particle energies ε_i are given by

$$\varepsilon_1 = \frac{\delta E_0}{\delta n_1} = \varepsilon_1^o + D_1 n_1 + U n_2, \quad \varepsilon_2 = \frac{\delta E}{\delta n_2} = \varepsilon_2^o + U n_1 + D_2 n_2, \tag{15}$$

where $i = 1, 2$ and $D_i = \Gamma_{ii}^{ii}$ and $U = \Gamma_{22}^{11} = \Gamma_{11}^{22}$. Note, the numbers n_1 and n_2 are integers in the usual case of the normal Hartree–Fock filling. Let us choose $\varepsilon_1^o < \varepsilon_2^o$. As seen from Equation (15), the normal occupation $n_2 = 0, n_1 = K$ persists if $\varepsilon_2^o + KU > \varepsilon_1^o + KD_1$. If this inequality does not hold, we can try another reasonable exercise, e.g., $n_1 = 0, n_2 = K$. But it also does not hold if $\varepsilon_2^o + KD_2 > \varepsilon_1^o + UK$. Thus, any Hartree–Fock filling fails provided

$$K(U - D_2) < (\varepsilon_2^o - \varepsilon_1^o) < K(D_1 - U). \tag{16}$$

In this case, we are forced to resort to the variational condition

$$\frac{\delta E_0}{\delta n_\lambda} = \mu \tag{17}$$

which implies $\varepsilon_1 = \varepsilon_2$. Then, after simple algebra one finds [28]

$$n_1 = [\varepsilon_2^o - \varepsilon_1^o + K(D_2 - U)]/Z \quad n_2 = [\varepsilon_1^o - \varepsilon_2^o + K(D_1 - U)]/Z, \tag{18}$$

with $Z = D_1 + D_2 - 2U$ being positive. We see that both n_1 and n_2 differ from 0 simultaneously if Equation (16) is valid. The energy obtained as a result of the rearrangement is $\delta E_{FC} = -[\varepsilon_1^o - \varepsilon_2^o + K(D_1 - U)]^2/2Z$. The analysis can easily be extended to a larger number of individual particle levels. The energy δE_{FC} is relatively small, but this effect could, in principle, help stabilize heavy and superheavy nuclei. The main feature of the obtained solution is the forced "collapse" of the distances between the energies of individual particles ε_i of the levels involved. Nowhere in the analysis was it assumed that the input parameters are small, and if this is so, then the Fermi liquid approach is applicable to the study of the FC, and not the Hartree–Fock method. The results obtained can be applied to a completely different problem if one associates n_i in Equation (15) with occupation numbers for the site i. Then, omitting the diagonal contribution D_i and taking $U > 0$ we arrive at the Coulomb gap problem and obtain ordinary results: the density of states at the Fermi surface falls [32]. The collapse of distances between different levels occurs if we add repulsion at the same site, i.e., assume $D_i \neq 0$, so as to ensure that Equation (16) is satisfied. This case, which has much in common with Hubbard's model, has not yet been studied.

3.2. Macroscopic Systems

Turning to macroscopic systems where T exceeds the splitting between levels, it is worth noting that the quasiparticle picture of the FC state is valid for superfluid systems with FC due to the presence of the gap in the spectrum of $E(p)$. Thus, only the case $T_c < T < T_f^0$ should be analyzed, where T_f^0 is the temperature at which the influence of the FC state on the properties of the system disappears [16,18,25,28]. In this case, calculations were carried out in [27], and it turns out that the width of quasiparticles $\gamma_{FC}(T)$ diverges at low T as $1/T$. From this result follows the conclusion $\gamma_{FC} >> \varepsilon_{FC}(p)$, which apparently destroys the quasiparticle picture of the phenomenon. Unfortunately, taking into account the huge enhancement of the effective mass $M_{FC}^* \sim T^{-1}$, the author [27] neglected the inverse suppression effect in the scattering amplitude Γ, responsible for the decay of quasiparticles. Here, we briefly present the results of an improved estimate of the width $\gamma_{FC}(T)$ [28]. To find $\gamma_{FC}(T)$ in a three-dimensional system, we use the well-known LFL equation [33]

$$\gamma_{FC}(T) \sim M^{*3} T^2 < \frac{W(\theta, \phi)}{\cos(\theta/2)} > . \tag{19}$$

Here, $W(\theta,\phi) \sim |\Gamma^2|$ is the transition probability, which depends on the angle θ between the vectors $\mathbf{p}_1$ and $\mathbf{p}_2$ of incoming particles and the angle ϕ between the planes defined by the vectors $\mathbf{p}_1, \mathbf{p}_2$ and $\mathbf{p}_1', \mathbf{p}_2'$. The brackets $< ... >$ denote angular averaging. In perturbation theory, Γ represents the interaction potential V. The result $\gamma_{FC} \sim T^{-1}$ [27] is obtained from (19):

$$M^*_{FC}(T) \simeq p_f(p_f - p_i)/T. \tag{20}$$

Here, we used the estimate $dn_0(p)/dp \simeq (p_f - p_i)^{-1}$). Thus, we infer that the effective mass $M^*_{FC}(T)$, as well as the density of states at the Fermi surface $N_F = \rho(\varepsilon = \mu, T) = p_F M^*(T)/\pi^2$, are enormously enhanced at low T. Taking into account Equation (20) and $\Gamma = V$, we obtain that the quasiparticles cannot exist [27]. However, in FC systems the difference between Γ and V is as huge as the difference between M^*_{FC} and the LFL effective mass M^*_L. For clarity, consider the velocity-independent scalar part of Γ, which is associated with the Landau amplitude f as follows from [28]:

$$\Gamma(q,\omega,T) = \frac{f(q)}{(1 - f(q)\chi_L(q,\omega,T))}. \tag{21}$$

The Lindhard function χ_L is estimated for particles with effective mass M^*. At $\omega \sim T$ both of the real and imaginary parts of $\chi_L(q, \omega \sim T)$ are of the same order of value: $|\mathrm{Re}\chi_L(q, \omega \sim T)| \sim N_F = p_F M^*_{FC}/\pi^2 \sim T^{-1}$ and $|\mathrm{Im}\chi_L(q, \omega \sim T)| \sim M^{*2}\omega/\pi q \sim T^{-1}$. This fact makes it possible to neglect the 1 in the denominator in Equation (21) and one finds $|\Gamma(T)| \sim 1/N_F(T) \sim T$. Thus, the effective interaction between FC quasiparticles becomes weak and T-dependent; this is completely altered compared to the interaction potential V. The result $|N_F(T)\Gamma(T)| \sim 1$ holds for any strongly correlated system. Taking into account Equation (19) together with Equations (20) and (21), we are left with

$$\gamma_{FC}(T) \sim \frac{M^{*3}_{FC}T^2}{M^{*2}_{FC}} \sim T\frac{\rho_c}{\rho}. \tag{22}$$

We see that $\gamma_{FC}(T)/|\varepsilon_{FC}(p,T)| \sim \rho_c/\rho$, and so the quasiparticle model holds as long as $\rho_c << \rho$. We safely assume that the FC density ρ_c is small: $\rho_c/\rho << 1$. Taking into account other components of Γ does not change this conclusion [28]. The estimate (22) can be obtained in another way [28] from the formula for the width of $\gamma_{FC}(T)$, related to the decay of a quasiparticle with energy $\varepsilon(p)$ and momentum $p > p_F$ [33]:

$$\gamma = 2\pi\,\mathrm{Tr}\int |\Gamma(q,\omega)|^2 n(k)(1 - n(\mathbf{p}+\mathbf{q}))\delta(\omega_0 - \omega)\frac{d^3k\,d^3q}{(2\pi)^6}. \tag{23}$$

where $\omega = \varepsilon(\mathbf{p}+\mathbf{q}) - \varepsilon(k)$ is the transferred energy and $\omega_0 = \varepsilon(p) - \varepsilon(\mathbf{p}-\mathbf{q}) \sim T$ the decrease in the quasiparticle energy as a result of rescattering processes. Therefore, a quasiparticle with the energy $\varepsilon(p)$ decays into a quasi-hole $\varepsilon(k)$ and two quasiparticles $\varepsilon(\mathbf{p}-\mathbf{q})$ and $\varepsilon(\mathbf{p}+\mathbf{q})$. Here, $\omega = \varepsilon(\mathbf{p}+\mathbf{q}) - \varepsilon(k)$ is the transferred energy, and $\omega_0 = \varepsilon(\mathbf{p}) - \varepsilon(\mathbf{p}-\mathbf{q}) \sim T$ is the decrease in the quasiparticle's energy due to rescattering processes. As a result, the quasiparticle with energy $\varepsilon(p)$ decays into a quasi-hole $\varepsilon(k)$ and two quasiparticles $\varepsilon(\mathbf{p}-\mathbf{q})$ and $\varepsilon(\mathbf{p}+\mathbf{q})$. It should also be noted that $\mathbf{q}$ must satisfy the condition $p > |\mathbf{p}-\mathbf{q}| > p_F$, since the quasiparticle loses momentum and energy. Integrating over d^3k in Equation (13) yields $\mathrm{Im}\chi_L(q,\omega)$ [28]. As a result, it is possible to find

$$\gamma_{FC} = -\int\int |\Gamma(q,\omega_0)|^2 M^{*2}\omega\frac{q^2 dq dx}{2\pi^3}. \tag{24}$$

In evaluating this integral, we denote $t = \varepsilon(\mathbf{p}) - \varepsilon(\mathbf{p}-\mathbf{q}) \leq T$ and express the angular variable x in terms of t, which gives $dx = M^* dt/pq$. Integrating over t introduces an additional factor T into Equation (24). Remembering that $|\Gamma| \propto T$, we again obtain

$$\gamma_{FC}(T) \sim |\Gamma|^2 M^{*3} T^2 \sim T\frac{\rho_c}{\rho}. \quad (25)$$

It is again seen that in the case $\rho_c/\rho << 1$, the lifetime of the FC quasiparticles is large, despite the huge density of states, and the quasiparticle model of the FC is preserved. Thus, as is often the case, in perturbation theory a catastrophe occurs [27], whereas in HF metals and unconventional superconductors quasiparticles exist; see, e.g., [4,6,7]. Thus, Equation (25) agrees with the experimental facts that quasiparticles exist in strongly correlated metals. It is seen from Equation (25) that the resistivity $\rho(T) \propto T$; see, e.g., [28,34]. A detailed discussion of $\gamma_{FC}(T)$ taking into account the contribution of transverse zero sound and the formation of the resistivity $\rho(T) \propto T$ is given in [34,35], while the absence of the FC state leads to $\rho(T) \propto T^2$; see, e.g., [15].

4. Superconducting State with FC at Finite Temperatures

Now, we consider the superconducting state of unconventional superconductors within the framework of the FC theory [16,18]. It was experimentally shown that in HF metals the quasiparticles are well-defined excitations [6] and in the superconducting state of unconventional superconductors the elementary excitations are Bogoliubov quasiparticles (BQs), that is, the excitations are Bardeen–Cooper–Schrieffer-like [4,7,23,24]. Therefore, as we shall see, unconventional superconductors exhibit the same scaling behavior of the condensation energy E_Δ/γ as conventional superconductors [5].

The energy dispersion of single-particle excitations and the corresponding coherence factors as a function of momentum were measured on high-T_c cuprates ($Bi_2Sr_2Ca_2Cu_3O_{10+\delta}$, T_c = 108 K) by using high-resolution angle-resolved photoemission spectroscopy [4]. All the observed features qualitatively and quantitatively agree with the behavior of BQs in conventional superconductors predicted by the BCS theory [4,6,23,24]. This observation shows that the superconducting state of unconventional superconductors is BCS-like with BQs, and implies the basic validity of the BCS formalism in describing the superconducting state, and is closely related to the deformation of flat bands by the superconducting phase transition [9,25,28]. On the other hand, a number of properties, such as the maximum value of the superconducting gap Δ_1, high density of states, and other exotic properties, are beyond the scope of the BCS theory [12,18,25]. Below, we call electron (hole) liquids electronic. For $T < T_c$, the thermodynamic potential Ω of the electron liquid is determined by the expression (see, e.g., [15,24])

$$\Omega = E_0 - \mu N - TS, \quad (26)$$

In Equation (26), N is the quasiparticle density, μ is the chemical potential, and S is the entropy. The ground state energy $E_0[\kappa(\mathbf{p}), n(\mathbf{p})]$ of the electron liquid is an exact functional of the order parameter of the superconducting state $\kappa(\mathbf{p})$ and quasiparticle occupation numbers $n(\mathbf{p})$ [18,26]. Here, we assume that the electronic system is two-dimensional to describe the results of [4], and all the results can be transferred to the case of a three-dimensional system [18]. This energy is determined by the well-known equation of the theory of weak coupling superconductivity:

$$E_0 = E[n(\mathbf{p})] + \delta E_s. \quad (27)$$

Here, $E[n(\mathbf{p})]$ is the exact Landau functional determining the ground state energy of a normal Fermi liquid [15,18], and δE_s is given by

$$\delta E_s = \int \lambda_0 V(\mathbf{p}_1, \mathbf{p}_2) \kappa(\mathbf{p}_1) \kappa^*(\mathbf{p}_2) \frac{d\mathbf{p}_1 d\mathbf{p}_2}{(2\pi)^4}. \quad (28)$$

Here, $\lambda_0 V(\mathbf{p}_1, \mathbf{p}_2)$ is the pairing interaction, with λ_0 being the coupling constant. The quasiparticle occupation number's

$$n(\mathbf{p}) = v^2(\mathbf{p})(1 - f(\mathbf{p})) + u^2(\mathbf{p})f(\mathbf{p}), \tag{29}$$

and at finite temperatures the order parameter κ becomes

$$\kappa(\mathbf{p}) = v(\mathbf{p})u(\mathbf{p})(1 - 2f(\mathbf{p})). \tag{30}$$

While at $T = 0$ the order parameter reads

$$\kappa(\mathbf{p}) = \sqrt{n_0(\mathbf{p})(1 - n_0(\mathbf{p}))}. \tag{31}$$

Here, the coherence factors $u(\mathbf{p})$ and $v(\mathbf{p})$ obey the normalization condition

$$v^2(\mathbf{p}) + u^2(\mathbf{p}) = 1, \tag{32}$$

and are selected from the condition that the energy E_0 of the system is minimal for a given entropy S [15]. The distribution function $f(\mathbf{p})$ determines the entropy:

$$S = -2 \int [f(\mathbf{p}) \ln f(\mathbf{p}) + (1 - f(\mathbf{p})) \ln(1 - f(\mathbf{p}))] \frac{d\mathbf{p}}{4\pi^2}. \tag{33}$$

We assume that the pair interaction $\lambda_0 V(\mathbf{p}_1, \mathbf{p}_2)$ is weak and arises due to electron–phonon interaction. Minimizing Ω with respect to $\kappa(\mathbf{p})$ and using the definition $\Delta(\mathbf{p}) = -\delta\Omega/\kappa(\mathbf{p})$, we obtain the equation relating single-particle energy $\varepsilon(\mathbf{p})$ to the superconducting gap $\Delta(\mathbf{p})$:

$$\varepsilon(\mathbf{p}) - \mu \ = \Delta(\mathbf{p}) \frac{1 - 2v^2(\mathbf{p})}{2v(\mathbf{p})u(\mathbf{p})}. \tag{34}$$

Single-particle energy $\varepsilon(\mathbf{p})$ is determined by the Landau equation:

$$\varepsilon(\mathbf{p}) = \frac{\delta E[n(\mathbf{p})]}{\delta n(\mathbf{p})}. \tag{35}$$

Note that $E[n(\mathbf{p})]$, $\varepsilon[n(\mathbf{p})]$, and the Landau amplitude

$$F(\mathbf{p}, \mathbf{p}_1) = \frac{\delta E^2[n(\mathbf{p})]}{\delta n(\mathbf{p}) \delta(\mathbf{p}_1)} \tag{36}$$

are exact equations [26]. Minimizing Ω with respect to $f(\mathbf{p})$, and after some algebra, we obtain the well-known equation for the superconducting gap $\Delta(\mathbf{p})$:

$$\Delta(\mathbf{p}) = -\frac{1}{2} \int \lambda_0 V(\mathbf{p}, \mathbf{p}_1) \frac{\Delta(\mathbf{p}_1)}{E(\mathbf{p}_1)} (1 - 2f(\mathbf{p}_1)) \frac{d\mathbf{p}_1}{4\pi^2}. \tag{37}$$

Here, the excitation energy $E(\mathbf{p})$ is defined by the Bogoliubov quasiparticles:

$$E(\mathbf{p}) = \frac{\delta(E_{gs} - \mu N)}{\delta f(\mathbf{p})} = \sqrt{(\varepsilon(\mathbf{p}) - \mu)^2 + \Delta^2(\mathbf{p})}. \tag{38}$$

The coherence factors $v(\mathbf{p})$, $u(\mathbf{p})$ and the distribution function $f(\mathbf{p})$ are given by the usual equations:

$$v^2(\mathbf{p}) = \frac{1}{2}\left(1 - \frac{\varepsilon(\mathbf{p}) - \mu}{E(\mathbf{p})}\right); u^2(\mathbf{p}) = \frac{1}{2}\left(1 + \frac{\varepsilon(\mathbf{p}) - \mu}{E(\mathbf{p})}\right), \tag{39}$$

$$f(\mathbf{p}) = \frac{1}{1+\exp(E(\mathbf{p})/T)}. \tag{40}$$

Equations (34)–(40) are the traditional ones of the BCS theory [23,24], defining the superconducting state with BQs and the maximum value of the superconducting gap $\Delta_1 \sim 10^{-3}\varepsilon_F$ provided that it is assumed that the system in question has not passed FCQPT.

As we have seen in Section 2, at $T = 0$, the ground state of the flat band system is degenerate, and the occupation numbers $n_0(\mathbf{p})$ of the single-particle states belonging to the flat band are continuous functions of the momentum $\mathbf{p}$, in contrast to the standard LFL step from 0 to 1 at $p = p_F$, as seen from Figure 1. As a result, at $T = 0$ the superconducting order parameter $\kappa_0(p) = \sqrt{n_0(p)(1-n_0(p))} \neq 0$ in the region occupied by FC; see Equation (9) [18]. This property contrasts sharply with the standard LFL picture, where for $T = 0$ and $p = p_F$ the order parameter $\kappa(p)$ is necessarily zero; see Figure 1. Because of the fundamental difference between the single-particle spectrum of FC and the spectrum of the rest of the Fermi liquid, a system having FC is essentially a two-component system separated from the usual Fermi liquid by a topological phase transition [10,17,18]. The range L of momentum space adjacent to μ where FC is located is given by $L \simeq p_f - p_i$; see Figure 1. We note that Equations (8) and (9) imply that the gap Δ is a linear function of both λ_0 and $\kappa_0(p)$. Since $T_c \sim \Delta$, we conclude that $T_c \propto \kappa_0 \propto n_{FC} \propto \rho_s$. Here, n_{FC} is given by Equation (10), being the density of superconducting electrons ρ_s, and forming the FC state; see Figure 1. In the case of over-doped high-temperature superconductors, the topological FCQPT takes place at the critical doping x_c, that is, $x = x_c$, $n_{FC} \propto p_F(p_f - p_i) \propto x_c - x$, with $(p_f - p_i)/p_F \ll 1$ [18,36]; therefore, at temperature $T = 0$, the density of the superconducting electrons n_{FC} turns out to be considerably smaller than the total electron density n_{el}:

$$n_{FC} = \rho_s \ll \rho_{el}. \tag{41}$$

We note that Equation (41) is in good agreement with experimental facts, being in contradiction with the BCS result that states: at $T = 0$ the density of the superconducting electrons ρ_s coincides with the density of electrons ρ_{el}, $\rho_s = \rho_{el}$ [37,38].

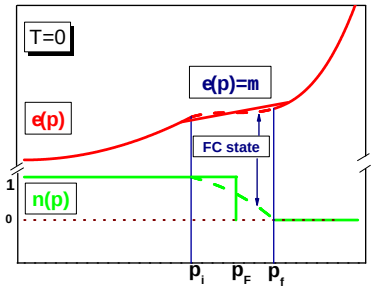

Figure 1. Schematic plot of electron liquid at $T = 0$ with FC and $\Delta_1 = 0$. In the case of a system without FC, the solid red curves show $\varepsilon(p)$, and $n_0(p)$ has the usual step function shown by the solid green line. Due to the presence of FC, the system is separated into two components: the first one is a normal Fermi liquid with the quasiparticle distribution function $n_0(p < p_F) = 1$, and $n_0(p > p_F) = 0$. The second one is FC with $0 < n_0(p_i < p < p_f) < 1$ and the flat single-particle spectrum $\varepsilon(p_i < p < p_f) = \mu$. Both of them are shown by the dashed lines. The Fermi momentum p_F satisfies the condition $p_i < p_F < p_f$.

Proceed to consider the superconducting state with FC that appears after the topological FCQPT point. At $T = 0$ and $\lambda_0 \to 0$ the maximum value of the superconducting gap is $\Delta_1 \to 0$, and also, the critical temperature $T_c \to 0$ and Equation (34) is converted into Equation (2) [16,18]. For $T \to 0$, Equation (2) defines a new Fermi liquid state with FC [16,17], that has a strong influence on the system properties up to temperature T_f^0, at which the influence of FC vanishes. It can be seen from Equation (2) that the entropy $S(T \to 0) \to S_0$, where $S_0 > 0$, is determined by the expression

$$S_0 = -\int [n_0(p)\ln n_0(p) + (1-n_0(p))\ln(1-n_0(p))]\frac{d\mathbf{p}}{(2\pi)^2}. \quad (42)$$

For $T \to 0$, Equation (2) defines a special state of a Fermi liquid with FC, for which the modulus of the order parameter $|\kappa(\mathbf{p})|$ has finite values in the $(p_f - p_i)$ region, whereas the maximum value of $\Delta_1 \to 0$ in this region. Observe that $f(\mathbf{p}, T \to 0) \to 0$, and it follows from Equations (29) and (30) that if $0 < n(\mathbf{p}) < 1$, then $|\kappa(\mathbf{p})| \neq 0$ in the region $(p_f - p_i)$. Such a state can be considered as superconducting, with an infinitely small value of Δ_1, so that the entropy of this state is equal to zero. At any finite $T > 0$, the entropy $S \geq S_0$, thus the topological FQCPT is of the first order [18]. The FC state is formed by the Landau interaction $F(p = p_F, p_1 = p_F)$ being relatively strong as compared with the pairing interaction $\lambda_0 V$; therefore, $\lambda_0 V$ does not noticeably disturb the occupation numbers n_0, but does disturb the corresponding flat band [9,18].

Consider the schematic $T - B$ phase diagram of an unconventional superconductor. As we shall see, this phase diagram differs significantly from that of conventional superconductors. However, this distinction does not exclude the common features of unconventional and traditional superconductors, which makes the physics of superconductivity more complex and attractive.

It is seen from the schematic phase diagram, Figure 2, that at temperatures $T \lesssim T_c$ the superconducting–normal phase transition shown by the solid line in Figure 2 is of the second order and entropy S is a continuous function of its variable T at $T_c(B)$. At temperatures $T \to 0$, the normal state can be recovered by the application of a magnetic field B that is approximately equal to the critical field $B \simeq B_{c2}$. This state can be considered as a magnetic field-induced LFL state since the resistivity exhibits LFL behavior, $\rho(T) \propto T^2$, which becomes $\rho(T) \propto T$ as the temperature increases [18]. When the system in its NFL state, under the application of a magnetic field $B > T^*$, HF metal transits to its LFL state, where temperature $T^*(B)$ defines the crossover midline, as seen from Figure 2. At $T \to 0$ the entropy of the superconducting state $S_{SC} \to 0$ and the entropy of the NFL state tends to some finite value $S_{NFL} \geq S_0$; see Equation (42). Thus, at temperatures $T_0 \geq T$ the equality $S_{SC}(T) = S_{NFL}(T)$ cannot be satisfied [18,39]. Thus, the second-order phase transition becomes the first below a certain temperature $T_0(B)$, as happens in $CeCoIn_5$ and as shown by the arrow in Figure 2 [39–41], while conventional superconductors do not exhibit a first-order phase transition under the influence of magnetic fields [15]. Note that the topological FCQPT is also the first-order phase transition. This first-order phase transition is determined by both the entropy jump mentioned above and the topological charge of FCQPT, which also changes by a jump [17,19]. Thus, possible fluctuations of the order parameter κ are excluded at $T \leq T_0$ [18,39].

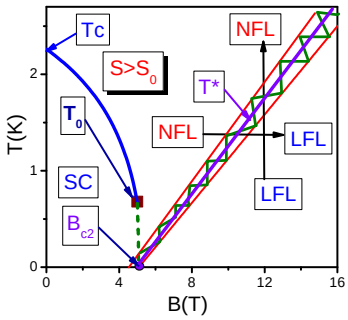

Figure 2. Schematic $T - B$ phase diagram of a superconducting HF metal, with upper critical field B_{c2}. The vertical and horizontal arrows crossing the transition region are marked with a line, representing the LFL–NFL and NFL–LFL transitions at fixed B and T, respectively. The shaded region shown by two adjacent red lines indicates the transition from the LFL state with $\rho(T) \propto T^2$ to the NFL state with $\rho(T) \propto T$. The median line T^* of the crossover is shown by the solid line. As shown by the solid curve, at $B < B_{c2}$ the system is in its superconducting (SC) state.

The superconducting critical field B_{c2} is shown by the purple circle. The superconducting–normal phase boundary is represented by the solid and dashed curves. The solid square indicates the point at $T = T_0$ at which the superconducting phase transition T_c changes from the second-order phase transition to the first-order phase transition.

5. General Behavior of the Scaled Condensation Energy of Conventional and Unconventional Superconductors

It can be seen from Equations (2) and (34) that the system is divided into two quasiparticle subsystems: the first subsystem in the range $(p_f - p_i)$ is characterized by quasiparticles with the effective mass $M^*_{FC} \propto 1/\Delta_1$, and the second is occupied by quasiparticles with the finite mass M^*_L and momenta $p < p_i$ [18]. The energy scale E_0 which defines the region occupied by quasiparticles with the effective mass M^*_{FC} is

$$E_0 = \varepsilon(\mathbf{p}_f) - \varepsilon(\mathbf{p}_i) \simeq 2\frac{(p_f - p_F)p_F}{M^*_{FC}} \simeq 2\Delta_1. \tag{43}$$

At $\lambda_0 \neq 0$, the gap Δ_1 is finite. It can be seen from Equation (37) that the superconducting gap depends on $\varepsilon(\mathbf{p})$. On the other hand, as seen from Equation (34), $\varepsilon(\mathbf{p})$ depends on $\Delta(\mathbf{p})$, since at $\Delta_1 \to 0$ the spectrum becomes flat. When differentiating both sides of Equation (34) relative to the momentum p, we find that the effective mass $M^*_{FC} = d\varepsilon(p)/dp\,_{|p=pF}$ reads [9]

$$M^*_{FC} \sim p_F \frac{p_f - p_i}{2\Delta_1}. \tag{44}$$

It follows from Equation (44) that the effective mass and the density of states $N(0) \propto M^*_{FC} \propto 1/\Delta_1$ are finite and constant at $T < T_c$, see Figure 3, [9,25]. Thus, we arrive at the result that contradicts the BCS theory, and follows from Equation (44):

$$\Delta_1 \propto T_c \propto V_F \propto \frac{1}{N(0)} \propto \frac{1}{M^*_{FC}}, \tag{45}$$

where $V_F \propto p_F/M^*_{FC}$ is the Fermi velocity [8,9,25]; see Figure 4. As $\lambda_0 \to 0$, the superconducting gap $\Delta_1 \to 0$ and the density of states near the Fermi level tends to infinity; see Equation (45).

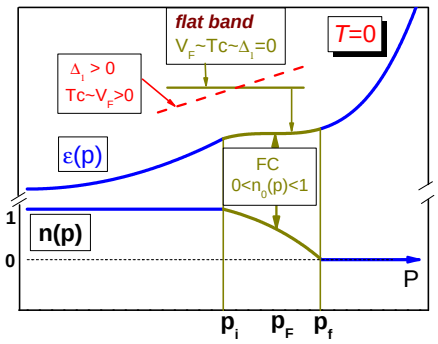

Figure 3. Schematic plot of electron liquid at $T = 0$ with FC. Because of the presence of FC, the system is divided into two components: the first is a normal Fermi liquid with a quasiparticle distribution function $n_0(p < p_i) = 1$ and $n_0(p > p_f) = 0$. The second is FC with $0 < n_0(p_i < p < p_f) < 1$ and a single-particle spectrum $\varepsilon(p_i < p < p_f) = \mu$. Due to the presence of FC, the Fermi momentum p_F satisfies the condition $p_i < p_F < p_f$. The modified flat band with $\Delta_1 > 0$ and $V_F > 0$, resulting from the emergence of the superconducting state, is shown by the red dashed line; see Equation (45). This change is depicted by the arrow and shown schematically by solid and dotted lines.

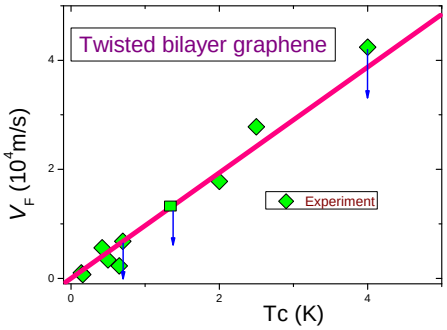

Figure 4. Experimental results for the average Fermi velocity V_F, shown as solid diamonds, as functions of critical temperature T_c for the magic-angle twisted bilayer graphene [8]. Down arrows indicate that $V_F \leq V_0$, where V_0 is the maximum value shown. The theory is shown by the solid line, which gives $V_F \propto T_c \propto 1/N(0)$; see Equation (45) [9].

Measurements of V_F as a function of T_c [8] are depicted in Figure 4. These observations are in good agreement with Equation (45). We note that this unusual behavior $T_c \propto 1/N(0)$ is observed in measurements on the uncommon superconductor $Bi_2Sr_2CaCu_2O_{8+x}$, where x is the oxygen doping concentration [9,42]; see Figure 5. Thus, our theoretical prediction [18,25] agrees very well with the experimental results [8,42]. It is worth noting that $V_F \to 0$, as well as $T_c \to 0$, as can be seen from Figure 4. This result shows that the flat band is disturbed by the finite value of Δ_1, and possesses a finite slope that makes $V_F \propto T_c$, as seen from Figure 4. Indeed, from Figure 4, the experimental critical temperatures T_c do not correspond to the minima in the Fermi velocity V_F as they would in any BCS-like theory [8]. This extraordinary behavior is explained within the framework of the FC theory based on the topological FCQPT forming flat bands [9,18]. As shown below, another unusual behavior, i.e., the general universal scaling of E_Δ/γ of both conventional and unconventional superconductors [5], is also associated with Equation (45) and explained within the framework of the FC theory.

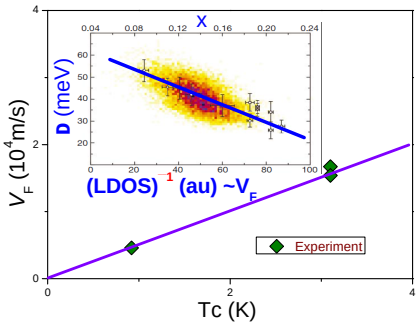

Figure 5. Experimental results for the mean Fermi velocity V_F as a function of the critical temperature T_c. The experiment is shown by filled diamonds [43–45]. The theory is shown by a solid line. The inset is taken from [42] and shows the experimental dependence of the superconducting gap on the integrated local density of states (LDOS) collected on the high-temperature superconductor $Bi_2Sr_2CaCu_2O_{8+x}$; x is the oxygen doping concentration. A more dark color represents more data points of the same integrated LDOS and the same gap size Δ [42].

We come to the conclusion that, in contrast to the traditional BCS theory of superconductivity, the single-particle spectrum $\varepsilon(\mathbf{p})$ strongly depends on the superconducting gap, and we have to solve Equations (35) and (37) in a consistent manner. On the other hand, suppose that Equations (35) and (37) are solved and the effective mass M^*_{FC} is determined. We can now fix $\varepsilon(\mathbf{p})$ by choosing the effective mass M^* of the system under consideration to be equal to M^*_{FC}, and then, solving Equation (37) in the same way as in the case of the

BCS traditional theory of superconductivity [23]. As a result, it can be seen that the superconducting state is characterized by BQs with the dispersion determined by Equation (38). The coherence coefficients v, u are determined by Equation (39), and the normalization condition (32) is satisfied. We conclude that the observed features are consistent with the BQ behavior according to experimental facts [4,5,7,42–46]. This observation suggests that a superconducting state with FC is similar to BCS and implies the basic reliability of BCS formalism when describing a superconducting state in terms of BQ. This is exactly the case that was observed experimentally in high-T_c cuprates; see, e.g., [4,7].

In fact, as is seen from Equations (43) and (44), even at $T = 0$, Fermi liquid with FC presenting a highly generated state is absorbed by the superconducting phase transition and never exhibits the dispersionless plateau associated with $M^*_{FC} \to \infty$. As a result, a Fermi liquid beyond the point of FCQPT can be described by two types of quasiparticles characterized by the two finite effective masses M^*_{FC} and M^*_L, respectively, and by the intrinsic energy scale E_0 [18,25].

It is reasonably safe to suggest that we have come back to the Landau theory by integrating out high-energy degrees of freedom and introducing quasiparticles. The sole difference between the Landau Fermi liquid and Fermi liquid having undergone FCQPT is that we have to expand the number of relevant low-energy degrees of freedom by adding both a new type of quasiparticle with effective mass M^*_{FC}, given by Equation (44), and the energy scale E_0, given by Equation (43). We have also to bear in mind that the properties of these new quasiparticles of Fermi liquid with FC cannot be separated from the properties of the superconducting state. It can be said that the system of quasiparticles in the range of L_{FC} becomes very "soft" and should be considered as a strongly correlated fluid. Thus, the properties and dynamics of the system are determined by a strong collective effect, which has its origin in the topological FCQPT and is determined by the macroscopic number of quasiparticles in the range L_{FC}. This system cannot be disturbed by scattering of the microscopic number of quasiparticles and represents a quantum protectorate [25,47]. We have returned to the theory of Landau Fermi liquids, since the high-energy degrees of freedom are eliminated and quasiparticles are returned. The only difference between LFL, which serves as the basis for constructing a superconducting state, and a Fermi liquid with FC is that we must expand the number of corresponding low-energy degrees of freedom, introducing a new type of quasiparticle with the effective mass of M^*_{FC}, given by Equation (44) and the energy scale E_0, indicated by Equation (43). Therefore, the single-particle spectrum $\varepsilon(\mathbf{p})$ is characterized by both two effective masses, M^*_L and M^*_{FC}, and by the scale E_0, which determine the low-temperature properties [18,25], while the dispersion of BQs is given by Equation (45). Note that both the effective mass M^*_{FC} and the scale E_0 are independent of temperature for $T < T_c$, where T_c is the critical temperature of the superconducting phase transition [18]. Obviously, we cannot directly relate these new quasiparticle excitations of BQs to quasiparticle excitations of an ideal Fermi gas, since the system in question has undergone topological FCQPT. However, the main properties of the LFL theory are preserved in FCQPT: low-energy excitation of a strongly correlated fluid with FC quasiparticles, whereas in the superconducting state they are represented by BQs [18]. It can be said that the system of quasiparticles in the range $(p_f - p_i)$ becomes very flexible and must be tuned in accordance with the superconducting state; see Equations (44) and (45).

At the same time, one could expect serious deviations from the BCS results when calculating the pairing correction ΔE_{FC} to $E_0[n]$. Applying the Landau formula for the change in $E_0[n]$ due to the variation $\delta n(\mathbf{p}, T) = n(\mathbf{p}, T) - n_0(\mathbf{p})$ of the occupation numbers [15] and adding the superfluid term (28), we arrive at the following result:

$$\Delta E_{FC} = \int (\varepsilon(\mathbf{p}) - \mu)\delta n(\mathbf{p}) \frac{d\mathbf{p}}{(2\pi)^2} + \delta E_s. \tag{46}$$

Here, δE_s is given by Equations (3), (28), and (31):

$$\delta E_s = -\frac{1}{2}\int_{p_i}^{p_f} \Delta_0(p)\sqrt{n_0(p)(1-n_0(p))}\frac{d\mathbf{p}}{(2\pi)^2}. \quad (47)$$

In the usual BCS case, the first term and the second one become proportional $\sim \Delta^2/\varepsilon_F^0$, so that $\Delta E_{FC} \sim \Delta^2/\varepsilon_F^0$ [15]. One could suspect that in a system with FC, the first term in Equation (46) turns out to be zero, for $\varepsilon(\mathbf{p}) - \mu = 0$ in the region $p_f - p_i$; see Equation (2). This is incorrect, since both the inverse Fermi velocity $1/V_F$ and the effective mass M_{FC}^* become finite under the influence of the superconducting state [9]; see Equation (45). Considering also that we are dealing with BQs, we are left with the usual BCS result for the superconducting condensation energy E_Δ, which is valid for both conventional superconductors and unconventional superconductors:

$$\Delta E_{FC}/\gamma \sim E_\Delta/\gamma \sim \frac{N(T)\Delta_1^2}{\gamma(T)} \sim \Delta_1^2 \sim T_c^2. \quad (48)$$

Here, $N(T)$ and $\gamma(T)$ are the density of states and the Sommerfeld coefficient, respectively. Experimental facts show that $N(T)$ and $\gamma(T)$ strongly depend on temperature T [12,18] and Δ_1 is the maximum value of the superconducting gap. However, $M^*(T) \propto N(T) \propto \gamma(T)$ [18], and we obtain $E_\Delta/\gamma \sim T_c^2$. It is seen from Figure 6 that Equation (48) is in accordance with experimental facts [5]. Indeed, taking into account that BQs of unconventional superconductors within the framework of the FC theory coincide with BQs of conventional superconductors and Equation (44), we conclude that the condensation energy E_Δ/γ given by Equation (48) has a universal form valid in the case of both conventional superconductors and unconventional ones. To check this conclusion, we compare our theoretical result with experimental facts [5]. Figure 6 shows the scaling of the condensation energy E_Δ versus T_c^2 on a log–log scale. It is seen from Figure 6 that the universal scaling $E_\Delta/\gamma \propto T_c^2$ is valid for all superconductors, both the conventional and the unconventional ones. This universal scaling behavior takes place over almost seven orders of magnitude for E_Δ/γ and three orders of magnitude for T_c [5]. This observation is not surprising since, as we have seen above, unconventional superconductors have the same BQs as conventional ones since the shape of the corresponding bands correlates with their T_c, as follows from Equation (45). Note that due to the strong influence of the pseudogap state on the properties of unconventional superconductors, such as the density of states, heat capacity, and even the true value of T_c, only optimally doped samples [5,48] were considered. Thus, the FC theory allows us to justify Equation (48), which describes superconductivity far beyond the weak coupling regime and is applicable to both conventional and unconventional strongly correlated superconductors.

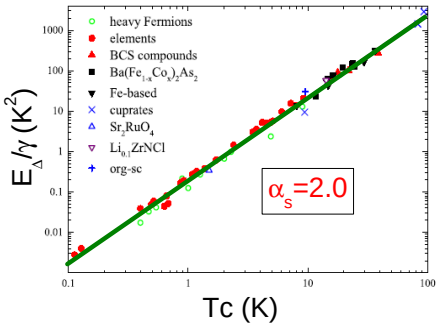

Figure 6. Condensation energy $E_\Delta/\gamma \propto T_c^2$ divided by specific heat γ as a function of T_c for a wide range of superconductors, with slope $\alpha_s = 2$ [5]; see Equation (48). The deviations from the best-fit line, spanning six orders of magnitude for E_Δ/γ and almost three orders of magnitude for T_c, are relatively small.

6. Summary

We analyzed the general behavior of unconventional superconductors and conventional superconductors and demonstrated that both the universal condensation energy scaling $E_\Delta/\gamma = N(0)\Delta_1^2/\gamma$ and the quasiparticle model are equally applicable to both types of superconductivity. Our explanation is based on the general properties of superconductors: Bogoliubov quasiparticles act in conventional and non-conventional superconductors, while the corresponding flat band is only deformed by the non-conventional superconducting state, making the effective mass finite. As a result, the non-conventional superconducting state becomes BCS-like. These observations suggest that in some cases the non-traditional superconducting state can be considered an analogue of the BCS state, as predicted in 2001. Note that in the normal state, non-traditional superconductors exhibit resistivity behavior $\rho(T) \sim T$, while traditional ones have $\rho(T) \sim T^2$. We also considered the superconducting electron density ρ_s of both superconductors. Our theoretical observations are in good agreement with experimental facts. Note that the theory of unconventional superconductivity is under development and new experimental results could be obtained that could reveal, for example, the absence of quasiparticles. Such observations may demonstrate the inconsistency of our explanation and lead to new considerations. However, for now our theoretical observations are in good agreement with experimental facts, demonstrating the existence of Bogoliubov quasiparticles and the scaling behavior of the scaled condensation energy.

Author Contributions: V.R.S. and A.Z.M. designed the project and directed it with the help of S.A.A.; V.R.S. and A.Z.M. wrote the manuscript and all authors commented on it. The manuscript reflects the contributions of all authors. All authors have read and agreed to the published version of the manuscript.

Funding: This work was supported by U.S. DOE, Division of Chemical Sciences, Office of Basic Energy Sciences, Office of Energy Research, AFOSR.

Institutional Review Board Statement: Not applicable.

Informed Consent Statement: Not applicable.

Data Availability Statement: The original contributions presented in the study are included in the article, further inquiries can be directed to the corresponding author.

Acknowledgments: We thank V.A. Khodel for fruitful discussions.

Conflicts of Interest: The authors declare no conflicts of interest.

References

1. Regnault, N.; Xu, Y.; Li, M.-R.; Ma, D.-S.; Jovanovic, M.; Bernevig, B.A.; Yazdani, A.; Cava, R.J.; Ong, N.P.; Schoop, L.M.; et al. Catalogue of flat-band stoichiometric materials. *Nature* **2022**, *603*, 824. [CrossRef] [PubMed]
2. Coleman, P.; Pèpin, C.; Si, Q.; Ramazashvili, R. How do Fermi liquids get heavy and die? *J. Phys. Condens. Matt.* **2001**, *13*, R723. [CrossRef]
3. Chen, L.; Lowder, D.T.; Bakali, E.; Andrews, A.M.; Schrenk, W.; Waas, M.; Natelson, D.; Setty, C.; Si, Q.; Sur, S.; et al. Shot noise in a strange metal. *Science* **2023**, *382*, 907. [CrossRef] [PubMed]
4. Matsui, H.; Sato, T.; Takahashi, T.; Wang, S.-C.; Yang, H.-B.; Ding, H.; Fujii, T.; Watanabe, T.; Matsuda, A. BCS-like Bogoliubov Quasiparticles in High-T_c Superconductors Observed by Angle-Resolved Photoemission Spectroscopy. *Phys. Rev. Lett.* **2003**, *90*, 217002. [CrossRef] [PubMed]
5. Kim, J.S.; Tam, G.N.; Stewart, G.R. Universal scaling law for the condensation energy across a broad range of superconductor classes. *Phys. Rev. B* **2015**, *92*, 224509. [CrossRef]
6. Hunter, A.; Beck, S.; Cappelli, E.; Margot, F.; Straub, M.; Alexanian, Y.; Tamai, A.; Zingl, M.; Mravlje, J.; Georges, A.; et al. Fate of Quasiparticles at High Temperature in the Correlated Metal Sr_2RuO_4. *Phys. Rev. Lett.* **2023**, *131*, 236502. [CrossRef]
7. Xu, K.-J.; Guo, Q.; Hashimoto, M.; Li, Z.-X.; Chen, S.-D.; He, J.; Shen, Z.X.; Tjernberg, O.; Lee, D.-H.; Lu, D.-H.; et al. Bogoliubov quasiparticle on the gossamer Fermi surface in electron-doped cuprates. *Nat. Phys.* **2023**, *19*, 1834. [CrossRef]
8. Qin, W.; Zou, B.; MacDonald, A.H. Critical magnetic fields and electron pairing in magic-angle twisted bilayer graphene. *Phys. Rev. B* **2023**, *107*, 024509. [CrossRef]
9. Shaginyan, V.R.; Msezane, A.Z.; Amusia, M.Y.; Japaridze, G.S. Effect of superconductivity on the shape of flat bands. *Europhys. Lett.* **2022**, *138*, 16004. [CrossRef]
10. Volovik, G.E. From standard model of particle physics to room-temperature superconductivity. *Phys. Scr.* **2015**, *T164*, 014014. [CrossRef]

11. Khodel, V.A.; Clark, J.W.; Zverev, M.V. Topological disorder triggered by interaction-induced flattening of electron spectra in solids. *Phys. Rev. B* **2020**, *102*, 201108. [CrossRef]
12. Amusia, M.Y.; Shaginyan, V.R. *Strongly Correlated Fermi Systems: A New State of Matter*; Springer Tracts in Modern Physics; Springer Nature: Cham, Switzerland, 2020; Volume 283.
13. Törmä, P.; Peotta, S.; Bernevig, B.A. Superconductivity, superfluidity and quantum geometry in twisted multilayer systems. *Nat. Rev. Phys.* **2022**, *4*, 528. [CrossRef]
14. Cao, Y.; Fatemi, V.; Fang, S.; Watanabe, K.; Taniguchi, T.; Kaxiras, E.; Jarillo-Herrero, P. Unconventional superconductivity in magic-angle graphene superlattices. *Nature* **2018**, *556*, 43. [CrossRef]
15. Lifshitz, E.M.; Pitaevskii, L. *Statistical Physics, Part 2*; Butterworth-Heinemann: Oxford, UK, 2002.
16. Khodel, V.A.; Shaginyan, V.R. Superfluidity in system with fermion condensate. *JETP Lett.* **1990**, *51*, 553.
17. Volovik, G.E. A new class of normal Fermi liquids. *JETP Lett.* **1991**, *53*, 222.
18. Shaginyan, V.R.; Amusia, M.Y.; Msezane, A.Z.; Popov, K.G. Scaling behavior of heavy fermion metals. *Phys. Rep.* **2010**, *492*, 31. [CrossRef]
19. Heikkila, T.T.; Volovik, G.E. *Flat Bands as a Route to High-Temperature Superconductivity in Graphite*; Springer Series in Materials Science; Springer Nature: Cham, Switzerland, 2016; Volume 244.
20. Rosenzweig, P.; Karakachian, H.; Marchenko, D.; Küster, K.; Starke, U. Overdoping Graphene beyond the van Hove Singularity. *Phys. Rev. Lett.* **2020**, *125*, 176403. [CrossRef]
21. Peri, V.; Song, Z.D.; Bernevig, B.A.; Huber, S.D. Fragile Topology and Flat-Band Superconductivity in the Strong-Coupling Regime. *Phys. Rev. Lett.* **2021**, *126*, 027002. [CrossRef] [PubMed]
22. Peotta, S.; Törmä, P. Superfluidity in topologically nontrivial flat bands. *Nat. Commun.* **2015**, *6*, 8944. [CrossRef]
23. Bardeen, J.; Cooper, L.N.; Schrieffer, J.R. Theory of superconductivity. *Phys. Rev.* **1957**, *108*, 1175. [CrossRef]
24. Bennemann, K.H.; Ketterson, J.B. *Superconductivity*; Springer: Berlin/Heidelberg, Germany, 2008.
25. Amusia, M.Y.; Shaginyan, V.R. Quasiparticle picture of high-temperature superconductors in the frame of a Fermi liquid with the fermion condensate. *Phys. Rev. B* **2001**, *63*, 224507 [.CrossRef]
26. Shaginyan, V.R. Quasiparticles in a strongly correlated liquid with the fermion condensate: Applications to high-temperature superconductors. *Phys. Lett.* **1998**, *A249*, 237. [CrossRef]
27. Nozières, P. Properties of Fermi liquids with a finite range interaction. *J. Phys. Fr. I* **1992**, *2*, 443. [CrossRef]
28. Dukelsky, J.; Khodel, V.A.; Schuck, P.; Shaginyan, V.R. Fermion condensation and non Fermi liquid behavior in a model with long range forces. *Z. Phys. B* **1997**, *102*, 245. [CrossRef]
29. Takatsuka, T. Proton mixing in π0-condensed phase of neutron star matter. *Prog. Theor. Phys.* **1984**, *71*, 1432. [CrossRef]
30. Yang, S.; Gu, Z.-C.; Sun, K.; Sarma, S.D. Topological flat band models with arbitrary Chern numbers. *Phys. Rev.* **2012**, *B86*, 241112. [CrossRef]
31. Yang, M. Flat bands and high Chern numbers in twisted multilayer graphene. *J. Math. Phys.* **2023**, *64*, 111901. [CrossRef]
32. Efros, A.L.; Shklovskii, B.I. Coulomb gap and low temperature conductivity of disordered systems. *J. Phys.* **1975**, *C8*, L49. [CrossRef]
33. Pines, D.; Nozières, P. *Theory of Quantum Liquids*; W.A. Benjamin: New York, NY, USA, 1966.
34. Shaginyan, V.R.; Mezane, A.Z.; Zverev, M.V. Transport properties of strongly correlated Fermi systems. *Symmetry* **2023**, *15*, 2055. [CrossRef]
35. Shaginyan, V.R.; Msezane, A.Z.; Popov, K.G.; Clark, J.W.; Zverev, M.V.; Khodel, V.A. Magnetic field dependence of the residual resistivity of the heavy-fermion metal $CeCoIn_5$. *Phys. Rev. B* **2012**, *86*, 085147. [CrossRef]
36. Shaginyan, V.R.; Stephanovich, V.A.; Msezane, A.Z.; Japaridze, G.S.; Popov, K.G. The influence of topological phase transition on the superfluid density of overdoped copper oxides. *Phys. Chem. Chem. Phys.* **2017**, *19*, 21964. [CrossRef] [PubMed]
37. Božović, J.I.; He, X.; Wu, J.; Bollinger, A.T. Dependence of the critical temperature in overdoped copper oxides on superfluid density. *Nature* **2016**, *536*, 309. [CrossRef] [PubMed]
38. Zaanen, J. Superconducting electrons go missing. *Nature* **2016**, *536*, 282. [CrossRef]
39. Shaginyan, V.R.; Msezane, A.Z.; Stephanovich, V.A.; Kirichenko, E.V. Quasiparticles and quantum phase transition in universal low-temperature properties of heavy-fermion metals. *Europhys. Lett.* **2006**, *76*, 898. [CrossRef]
40. Bianchi, A.; Movshovich, R.; Oeschler, N.; Gegenwart, P.; Steglich, F.; Thompson, J.D.; Sarrao, J.L.; Pagliuso, P.G. First-Order Superconducting Phase Transition in $CeCoIn_5$. *Phys. Rev. Lett.* **2002**, *89*, 137002. [CrossRef] [PubMed]
41. Izawa, K.; Yamaguchi, H.; Matsuda, Y.; Shishido, H.; Settai, R.; Onuki, Y. Angular position of nodes in the superconducting gap of quasi-2D heavy-fermion superconductor $CeCoIn_5$. *Phys. Rev. Lett.* **2001**, *87*, 057002. [CrossRef]
42. Pan, S.H.; O'Neal, J.P.; Badzey, R.L.; Chamon, C.; Ding, H.; Engelbrecht, J.R.; Davis, J.C.; Ng, K.-W.; Hudson, E.W.; Lang, K.M.; et al. Microscopic electronic inhomogeneity in the high-T_c superconductor $Bi_2Sr_2CaCu_2O_{8+x}$. *Nature* **2001**, *413*, 282. [CrossRef]
43. Yankowitz, M.; Chen, S.; Polshyn, H.; Zhang, Y.; Watanabe, K.; Taniguchi, T.; Graf, D.; Young, A.F.; Dean, C.R. Tuning superconductivity in twisted bilayer graphene. *Science* **2019**, *363*, 1059. [CrossRef]
44. Lu, X.; Stepanov, P.; Yang, W.; Xie, M.; Aamir, M.A.; Das, I.; Urgell, C.; Watanabe, K.; Taniguchi, T.; Zhang, G.; et al. Superconductors, orbital magnets and correlated states in magic-angle bilayer graphene. *Nature* **2019**, *574*, 653. [CrossRef]
45. Stepanov, P.; Das, I.; Lu, X.; Fahimniya, A.; Watanabe, K.; Taniguchi, T.; Koppens, F.H.L.; Lischner, J.; Levitov, L.; Efetov, D.K. Untying the insulating and superconducting orders in magic-angle graphene. *Nature* **2020**, *583*, 375. [CrossRef]

46. Nakamae, S.; Behnia, K.; Mangkorntong, N.; Nohara, M.; Takagi, H.; Yates, S.J.C.; Hussey, N.E. Electronic ground state of heavily overdoped nonsuperconducting $La_{2-x}Sr_xCuO_4$. *Phys. Rev. B* **2003**, *68*, 100502. [CrossRef]
47. Laughlin, R.B.; Pines, D. The middle way. *Proc. Natl. Acad. Sci. USA* **2000**, *97*, 28. [CrossRef] [PubMed]
48. Loram, J.W.; Mirza, K.A.; Wade, J.M.; Cooper, J.R.; Liang, W.Y. The electronic specific heat of cuprate superconductors. *Phys. C* **1994**, *235–240*, 134. [CrossRef]